HHS Public Access

Author manuscript

Ecotoxicol Environ Saf. Author manuscript; available in PMC 2023 March 29.

Published in final edited form as:

Ecotoxicol Environ Saf. 2022 August ; 241: 113800. doi:10.1016/j.ecoenv.2022.113800.

A comparative proteomics study of *Arabidopsis thaliana* responding to the coexistence of BPA and TiO_2-NPS at environmentally relevant concentrations

Huiming Huang[a,b], **Brian Grajeda**[c,d], **Cameron C. Ellis**[c,d], **Igor L. Estevao**[c,d], **Wen-Yee Lee**[b,*]

[a]Institute of Subtropical Agriculture, Fujian Academy of Agricultural Sciences, Jiulong Ave, Zhangzhou, Fujian 363005, China

[b]Department of Chemistry and Biochemistry Department, The University of Texas at El Paso, 500 West University Avenue, El Paso, TX 79968, United States

[c]Department of Biological Sciences, The University of Texas at El Paso, 500 West University Avenue, El Paso, TX 79968, United States

[d]Border Biomedical Research Center (BBRC), The University of Texas at El Paso, 500 West University Avenue, El Paso, TX 79968, United States

Abstract

Through the applications of recycling sewage sludge to soils as nutrients, bisphenol A (BPA) and titanium dioxide nanoparticles (TiO_2-NPs) are commonly found in the agricultural environment. Previous studies have reported that BPA and nanoparticles are harmful to the environment. However, the combined toxicity of both compounds is not yet understood. This work presented an in-depth proteomic analysis of *Arabidopsis thaliana* exposed to BPA and TiO_2-NPs concurrently at environmentally relevant levels. Seeds were simultaneously treated with varying concentrations of BPA (0, 10, 100, and 1000 μg·kg^{-1}) and TiO_2-NPs (0, 1, 10 and 100 mg·kg^{-1}). In treatment of 1000 μg·kg^{-1} BPA and 100 mg·kg^{-1} TiO_2-NPs, highest seed germination rate (87.97%, $p < 0.05$) was observed. Shorter primary roots but more branched roots were obtained in treatments of high BPA and NPs concentrations (100, 1000 μg·kg^{-1} BPA and ^{1}0, 100 mg·kg^{-1} TiO_2-NPs) while no significant effects on plant height and biomass were found. In the comparative analysis, both concentration related positive and negative effects were observed, such as regulation of cell proliferation (positive), root hair elongation (positive), cellular response to oxidative stress (negative), and cell wall organization (negative). In response to the stress caused by BPA and

*Corresponding author. wylee@utep.edu (W.-Y. Lee).

CRediT authorship contribution statement

Huiming Huang: Methodology, Formal analysis, Writing, Visualization, Data curation. **Brian Grajeda:** Methodology, Formal analysis, Writing, Visualization. **Cameron C. Ellis:** Methodology, Writing. **Igor L. Estevao:** Methodology, Writing. **Wen-Yee Lee:** Conceptualization, Resources.

Declaration of Competing Interest

The authors declare that they have no known competing financial interests or personal relationships that could have appeared to influence the work reported in this paper.

Appendix A. Supporting information

Supplementary data associated with this article can be found in the online version at doi:10.1016/j.ecoenv.2022.113800.

TiO2-NPs, some proteins related to plant root development, such as CD48E, DNAJ2 and GL24, were up-regulated explaining the shorter primary root length and more branched roots. Moreover, *Arabidopsis* may have stimulated its ability of resource transportation and energy metabolism to overcome the stress and maintain or somehow enhance their growth by up-regulating proteins like TBB6, CALM1, RAA2A, G3PP2 and KASC1. Our comparative proteomics analysis also highlighted multiple biological processes that consequently lead to the stability of plant growth and its stress adaptation. The results demonstrated that applying biosolids to soil as a fertilizer may be considered as a sustainable practice.

Keywords

Bisphenol A; Titanium dioxide nanoparticles; *Arabidopsis thaliana* ; Proteomics; LC-MS/MS

1. Introduction

Biosolid from wastewater sludge is often applied to soils as a fertilizer for recycling of nutrients, soil health enhancement and land restoration to improve and stimulate plant growth (Colón et al., 2017). About 7.2 million tons of biosolids (dry mass) are generated in the U.S. per year. Of those, 55% (about 3.9 million) were applied to soil (Verslycke et al., 2016). In European countries, the number is about 2.4 million dry tons of biosolids generated per year (Chang et al., 2001). Even though it was considered an important biological resource for sustainable agriculture and economic practices, the disadvantage of biosolid application in agriculture is their pollutant load. Previous studies have documented that biosolids contain many contaminants of emerging concern (CECs), including endocrine-disrupting chemicals (EDCs) (Giudice and Young, 2011), heavy metals (Yang et al., 2014), organic compounds (Torri and Alberti, 2012), pharmaceuticals (García-Santiago et al., 2016), and nanoparticles (NPs) (Bellani et al., 2020). Particularly, Bisphenol A (BPA) (Petrie et al., 2019) and titanium dioxide nanoparticles (TiO_2-NPs) (Gottschalk et al., 2009b) are commonly found in the sludge and could affect the plant growth and its bio-system.

BPA toxicity was reported on mung bean by inhibiting shoot and root development, and decreasing chlorophyll content, stomata size, and photosynthetic activity (Kim et al., 2018). Wang et al. (2015a) studied the mechanism of BPA effects on soybean growth and reported that BPA could regulate levels of growth and stress hormones in plant roots in a dose-dependent manner. Treatment with BPA concentration at 1.5 $mg{\cdot}L^{-1}$ improved soybean seedling growth, while at high concentrations (3–96 $mg{\cdot}L^{-1}$) BPA inhibited seedling growth (Wang et al., 2015b).

Nanoparticles have high surface reactivity and large surface area and are capable of amalgamating with other pollutants and get absorbed into the organism, which is accompanied with interactive effects such as bioconcentration enhancement, endocrine disruption and developmental neurotoxicity (Fang et al., 2016; Guo et al., 2019). Reports have shown that engineered nano-materials exhibit an increasing occurrence in the environment and may cause toxicity to the ecosystem (Hu and Zhou, 2013). For instance, the wide usage of TiO_2-NPS in manufacturing and commercial products has increased their

levels in agricultural soils (Weir et al., 2012). Movafeghi et al. identified TiO_2-NPS uptake by the aquatic plant *Spirodela polyrrhiza*; subsequently, all the plant growth parameters were significantly decreased, and changes in antioxidant enzyme activities were observed with a significant increase of superoxide dismutase (Movafeghi et al., 2018). In a hydroponic study on *Nigella arvensis* L. the results showed that TiO_2-NPS had an inhibiting effect in the high concentration greater than 1000 mg L^{-1} of TiO_2-NPS where the synthesis of chlorophylls and carotenoid was reduced, while a stimulating effect at the low concentrations of 50 and 100 mg L^{-1} was observed (Chahardoli et al., 2022). On the other hands, TiO_2-NP could also be beneficial to plants. Mahmoodzadeh et al. reported the elevated levels of germination and improved radicle and plumule development in canola seedlings when treated with TiO_2 NPs application (1200 and 1500 mg L^{-1}) (Mahmoodzadeh et al., 2013). Shah et al. found that 60 ppm (mg Kg^{-1}) TiO_2-NPS treatment effect positively on the rate of germinate and growth of maize seedling under salinity stress. (Shah et al., 2021). Wang el al has reported that the aged hydrophobic and hydrophilic-coated nano TiO_2-NPS induced more positive effects on carrot plant (*Daucus carota* L.) development at 100 and 400 mg Ti/kg soil when compared with control. (Wang et al., 2021).

While many studies are focused on BPA or TiO_2-NPS, there is a lack of information regarding the effect on plants when both materials are present. Therefore plant responses to these environmental stressors are largely unknown. In this study, we aimed to investigate the changes of plant proteome as well other biological parameters, such as seed germination, root growth, and plant heights and masses, under the exposure to both BPA and TiO_2-NPS. The model plant, *Arabidopsis thaliana* was utilized due to its simple and convenient genome information (The Arabidopsis Genome, 2000). An insight into the molecular mechanisms associated with BPA and TiO_2-NPS in the model plant *Arabidopsis thaliana* roots is herein presented.

2. Materials and methods

2.1. Plant culture and exposure

Analytical grade (> 98%, Cat no. 80057) BPA was obtained from Sigma-Aldrich (Missouri, US). Anatase TiO_2-NPS (15 nm average particle size, Cat no. 82021–366) and agar powder (Cat no. 41106212) were purchased from Alfa Aesar, Thermo Fisher Scientific Chemicals, Inc. Murashige & Skoog, MS Medium (Cat no. M10200–50) were used as culture medium and purchased from Research Products International Corp. Wild-type *Arabidopsis thaliana* seeds, Ecotype Columbia, (Cat no. 470112–764) were obtained from the Biotechnology Education Company, ED VOTEK.

Plant growth analysis were performed in response to BPA and TiO_2-NPs at different concentrations. BPA stock solution was prepared at 100 mg·L^{-1} in analytical grade ethanol and a stock of TiO_2-NPS solution was prepared at 1 g·L^{-1} in deionized water (DI, Milli-Q water purification system). During each treatment preparation, TiO_2-NPS stock suspensions were diluted and homogenized in an ultrasonic bath for 30 min before use. In this study we used environmentally relevant levels of BPA ranging from 10 to 1000 μg·kg^{-1} and TiO_2-NPs concentrations from 1 to 100 mg·kg^{-1} in agar media under five treatments (shown in Table 1).

The agar media used in the treatment and control groups were supplemented with culture medium (Weigel and Glazebrook, 2002) (400 mL 1 × MS medium with 0.6% (g/g) agar powder). As an example, the preparation for treatment G3 (i.e., 10 μg·kg^{-1} BPA and 1 mg·kg^{-1} TiO_2-NPS) is described as follows. One milliliter of the stock BPA solution was firstly diluted into 100 mL with DI to get a 1 mg·L^{-1} working solution. Then, 4 mL of this BPA working solution and 0.4 mL stock TiO_2-NPS along with 2.4 g of agar powder were added into culture medium to have a final mass of 400 g of agar media.

2.2. Plant germination and growth conditions

For the germination experiment, the *Arabidopsis thaliana* seeds were firstly with bleach solution (30% commercial bleach) for 15 min, washed 3 times with sterile water and vernalized at 4°C for 2 days. Then seeds were evenly sown in petri dishes with a culture medium using 100 seeds per treatment group. The germination rates were counted every day for seven days and primary root lengths were measured at 7 and 14 days after seed sowing.

After germination, 30 *Arabidopsis thaliana* plants per treatment were transplanted into glass jars with agar media and put into a pre-sterilized growth chamber using 75% isopropanol for five weeks. Parameters of the chamber were set with 16 h/8 h day/night period, at 25/22 °C day/night temperature, and 65–70% relative humidity. Plants were regularly watered with 1/4 MS medium solution every two days. For the first week, each jar was watered with 2 mL of the medium solution. The irrigation water volume was then gradually increased to 15 mL per jar until the 5th week to meet the need of plant growth.

After five weeks of growth period, *Arabidopsis thaliana* plants were harvested, plant heights were measured and plant biomasses in fresh weight were recorded. Plants were then divided into three parts: roots, leaves and stems which were immediately freezed in liquid nitrogen and stored at − 80 °C for further analysis.

2.3. Total protein extraction

After harvest, plants were carefully rinsed with DI to remove agar gel on the roots. Protein extraction by total protein extraction kit (G-Bio-sciences, Cat no. 82021–366) was performed. Briefly, cell lysis of plant roots was achieved by mixng 1 g of the root sample from the respective treatment and 2 mL of TPE Buffer-I. Samples were then transfered into a grinder to reach a homogeneous suspension. This preparation was carried out in ice to avoid excess heating and protein degradation. The homogenate was transferred to a 15 mL tube and 240 μl of TPE Buffer-II was added, vortexed immediately for 30 s, put in a boiling hot water bath for another 30 s, and vortexed again for 30 s. This heating and vortexing process (30 s each) was repeated until a clear solution was obtained. After 10 min of incubation in a boiling water bath, the extracts tubes were centrifuged for 10 min at 16,000 xg under − 4 °C. The supernatant was transferred to another clean protease free tube and stored at − 80 °C for further analysis.

2.4. Protein concentration and Tryptic digestion

Sample protein concentrations were measured by Bicinchoninic acid assay (BCA) according to manufacturer instructions (Pierce ™ BCA Protein Assay kit, cat no. 23227). After protein

concentration acquisition was performed, 100 μg of each protein sample obtained from the aforementioned step was used for protein digestion by a modified method (FASP Protein Digestion (Aguilera et al., 2020) Expedeon, cat no. 44250) to obtain peptides for analyses by mass spectrometry. Detailed preparation processed for each protein sample is described in Supplementary Information. Resulting tryptic peptides were frozen at − 80 °C for two hours and subsequently dried in a lyophilizer. Samples were re-suspended with 100 μl of 0.1% formic acid LCMC grade water solution for a final concentration of 1 $\mu g \cdot uL^{-1}$ prior to 1D LC-MS/MS analysis.

2.5. Proteomic analysis using 1D LC-MS/MS

One microliter of digested peptides (1 $\mu g \cdot \mu l^{-1}$) was injected to a custom packed AQUA 5 μm, 125 Å, C18 (Phenomenex, cat no. 04A-4299) 20 cm, 15 ± 1 μm, PicoFrit Emitter (New Objective) equilibrated with optima grade (ThermoFisher Scientific) 5% solvent B (90% acetonitrile, 0.1% formic acid) and 95% solvent A (0.1% formic acid). Detailed eluting parameters are described in Supplementary Information. The mass spectrometer was equipped with a NanoSprayFlex ion source (ThermoFisher Scientific). Peptides were analyzed in top 10 data dependent MS^2 acquisition by a Q-Exactive Plus Hybrid Quadrupole-Orbitrap mass spectrometer (ThermoFisher Scientific). Full scan parameters were set to 70,000 resolution, $3e^6$ AGC target, with a scan range of 350–1600 *m/z*. MS^2 parameters were set to 17,500 resolution, $1e^5$ AGC target, isolation window at 3.0 *m/z*, (N) CE: 30, charge exclusion: unassigned, 1, > 8.

2.6. Spectra data processing and database search

Proteomic data analysis was performed using the Proteome Discoverer (PD) v2.5.0.400 (Thermo Fisher Scientific), with an estimated false discovery ratio (FDR) of 1%. Common contaminants such as trypsin autolysis fragments, human keratins, and protein lab standards, were included as well as in house contaminants which may be found in the cRAP contaminant database. *Arabidopsis thaliana* was downloaded from UniProtKB; http://www.uniprot.org/ with 77,369 entries (Downloaded on October 9, 2019). The parameters used in the PD: HCD MS/MS were described in details in the Supplementary Information. A protein threshold of 99%, peptide threshold of 95%, and a minimum number of 2 peptides were used for protein validation. The software reports statistical significance proteins between each treatment group and control (Fisher's Exact Test at $p < 0.05$). ClustVis (Version December 2018) was used to perform a Principal Component Analysis (PCA) on the technical replicates from the Mass spectra (Metsalu and Vilo, 2015) as shown in the Supplementary Information (Fig. S2). The fold change significance cutoff value were set at Log2(fold-change)> 0.5 in all the comparisons. To visualize the protein expression changes with varying groups of treatments and control, a volcano plot was plotted by a data analysis and visualization online tool (http://www.bioinformatics.com.cn). The heat map was drawn after the expression was transformed into the fold-change to the mean expression of each protein in all treatments and control, due to the huge fold-changes difference of proteins.

2.7. GO functional, pathway enrichment and protein interaction network analysis

To comprehensively analyze the biological functions, gene ontology (GO) for proteins analysis was performed by the database of QuickGO (https://www.ebi.ac.uk/QuickGO/)

and the UniProt (https://www.uniprot.org/). The GO term analysis included the biological process, cellular component and molecular function.

STRING version 11.0 (https://string-db.org/) was used to analyze the protein interaction information (interaction network) of all significant differentially expressed proteins (SDEPs) and the Kyoto encyclopedia of genes and genomes (KEGG) pathways of their biological functions were also obtained. An illustration of the interaction network of these proteins was then generated.

3. Results and discussion

The concentrations of BPA and TiO_2-NP in this study were selected to be relevant to the levels found in the wastewater sludge, and presumably would not to cause severe toxicological effects in plant growth. Previous studies have shown that BPA concentrations in sewage treatment sludge ranged around 370 $\mu g \cdot kg^{-1}$ (Corrales et al., 2015; Mohapatra et al., 2011; Petrie et al., 2019) and TiO_2-NPs concentrations were reported between 20 $mg \cdot kg^{-1}$ to 136 $mg \cdot kg^{-1}$ (Gottschalk et al., 2009a, 2009b). Thus, in this study we used environmentally relevant levels of BPA ranging from 10 to 1000 $\mu g \cdot kg^{-1}$ and TiO_2-NPs concentrations from 1 to 100 $mg \cdot kg^{-1}$ for the treatments as shown in Table 1. Uncertain parameters in biosolids have been reported, such as organic matter (Simonin et al., 2021; Wu et al., 2017; Zhu et al., 2012) and soil colloid (Campos et al., 2020; Philippe et al., 2018; Sun and Zhou, 2015). In order to avoid the discrepancy, agar media were used for the treatment and control groups and supplemented with growth medium (Weigel and Glazebrook, 2002) (400 mL 1 × MS medium with 0.6% (g/g) agar powder). Furthermore, *Arabidopsis thaliana* was selected as the model plant for its complete genome information which is fully available online at UniProtKB; http://www.uniprot.org/.

3.1. Morphological and physiological response analysis

To investigate the effect of both BPA and TiO_2-NPs on *Arabidopsis thaliana* seeds germination, we first inspected the morphological responses daily within the first 7 days. Five treatments and control group (shown in Table 1) with 100 seeds in each group were set up. As shown in Fig. 1A and B, seeds started to germinate on day 2 and reach the peak of germination after day 5. It was also observed that seeds in group G5, with 100 $\mu g \cdot kg^{-1}$ BPA and no TiO_2-NPs, had the lowest germination rate (68.98%), while the highest germination rate (87.97%, $p < 0.05$) was obtained in G1, in which plants were treated with 1000 μg/kg BPA and 100 mg/kg TiO_2-NPs. As seeds in G1 and G2 have higher germination rates than G4 and G5, this indicates that the seed germination was positively affected by the coexistence of BPA and TiO_2-NPs. Positive effect of TiO_2-NPs exposure on plant seed germination had been reported on other plant species, such as spinach (Zheng et al., 2005), wheat (Feizi et al., 2012), canola (Mahmoodzadeh et al., 2013), and onion (Laware and Raskar, 2014). Due to the high specific surface area, nanoparticles may sequester nutrients on their surfaces and thus serve as a nutrient stock to seeds (Navarro et al., 2008). Secondly, nanomaterials could create layers of small pores on the seed coat, which facilitate for the water uptake process (Mahakham et al., 2017). TiO_2-NPs may also induce oxidation-reduction reactions by enhancing superoxide dismutase (SOD) and peroxidase

dismutase (POD) activities (Laware and Raskar, 2014) during seed germination, resulting in eliminating free radicals in seeds which would enhance the germination process.

In terms of root growth during seedling period, the coexistence of the two contaminates seemed to show negative effects (Fig. 1C and D). The plant roots in single component treatments, i.e. G5 (100 μg·kg^{-1} BPA and 0 TiO_2-NPs) and G4 (0 BPA and 10 mg·kg^{-1} TiO_2-NPs), grew longer and had smaller branched roots than those measured in the control. In higher concentrations of treatments (i.e. G1 and G2), shorter primary roots with more branched roots were obtained. The effects of BPA on plant root growth were related to BPA-induced changes in hormones (Li et al., 2018), such as single endogenous hormone, growth, and stress hormones (Wang et al., 2015a). Bahmani et al. (2020) found that BPA depressed *Arabidopsis* root growth by suppressing expansion expression and inducing auxin accumulation/redistribution which highly affects cell elongation and division (Bahmani et al., 2020).

After 5 weeks of cultivation, plant height and biomass were recorded. A significant difference in height with 49.2% higher compared to control was found in G3 (10 μg·kg^{-1} BPA and 1 mg·kg^{-1} TiO_2-NPs) and significantly more plant biomass with 13.8% compared to control was found in G4 (0 BPA and 10 mg·kg^{-1} TiO_2-NPs). Other treatments did not have significant effects on both plant height and biomass when compared to the control as shown in Fig. 1E and F.

It was clear that the impacts of BPA and TiO_2-NPS on seed germination and root growth did not affect the later plant morphology outcomes during the growth period (Fig.1 and Table S1). The levels of BPA and TiO_2-NPS used in this study also did not present to be toxic to the plants. This is an important observation for the following protein analysis. It should be noted that plants in G1, G2, and G3 showed signs of stress with more yellow leaves. However, they remained “healthy” in all treatments during the entire experiment period.

3.2. Comparative proteomics

After harvest, plant roots were carefully removed, and proteins was extracted and analyzed. A total of 1215 proteins were identified and quantified across all the treatment and control groups against *Arabidopsis thaliana* UniProt sequence database. In addition, 131 proteins (Table S2) were found significant differentially expressed as shown in the volcano plots in Fig. 2. Proteins in G1~G5 with red or blue colors were considered up-regulated or down-regulated respectively when compared to those of the control. As observed in Fig. 2, G1 (the highest levels of BPA and NPs) had the most up-regulated (64 proteins, red color) and down-regulated (49 proteins, blue color) proteins. Heatmap of significant differentially expressed proteins (SDEPs) were also shown in Fig. 3. The heatmap again reveal the most SDEPs found in G1 than other treatment groups.

We used Venn diagrams (Fig. 4) to further study the SDEPs identified in different treatment groups compared to the control. Of the 131 proteins identified, G1 vs. Control comparison has the most number of SDEPs with 113 proteins (64 up-regulated, 49 down-regulated, Fig. 4A and details shown in SI Table 3), indicating that the higher concentration of the mixed contaminants, the more proteins were affected in the plant system. Detailed protein

information is included in SI Table 4. As the proteins that were significantly up- or down regulated by BPA and TiO_2-NPS respectively, 13 SEDPs were identified in G4 (10 $mg \cdot kg^{-1}$ TiO_2-NPS only) vs. Control and 11 SEDPs were found in G5 (100 $\mu g \cdot kg^{-1}$ BPA only) vs. control (Fig. 4A). In G4 vs. control, two down-regulated protiens Glutathione S-transferase F2 (GSTF2) and Glutathione S-transferase F3 (GSTF3) were defense-related proteins during plant stress and they are responsible for binding a series of heterocyclic compounds and have a detoxification role against certain herbicides (Dixon et al., 2011; Loeffler et al., 2005); and Jacalin-related lectin 33 (JAL33) is a sugar-binding protein, which responses to carbohydrate binding (Takeda et al., 2008). Another 7 proteins were found up-regulated and they were chaperonin 60 subunit beta 2, chloroplastic (CPNB2, involved in protein assisted folding) (Bonshtien et al., 2009), cell division control protein 48 homolog E (CD48E, unctions in cell division and growth processes), protein TIC110, chloroplastic (TI110, involved in protein precursor import into chloroplasts), tubulin alpha-1 chain (TBA1, major constituent of microtubules), MEE5 (A0A178WHI8, similar to classic translation factor GTPase family), receptor for activated C kinase 1 C (GPLPC, involved in multiple hormone responses and developmental processes) (Guo and Chen, 2008), and Sucrose synthase 4 (SUS4, Sucrose-cleaving enzyme that provides UDP-glucose and fructose for various metabolic pathways) (Cheng et al., 2017). It should be noted that CPNB2, GPLPC, and CD48E were also found up-regulated in G2 vs. Control (Table S4). As G2 has the same level of TiO_2-NPS as G4, it could be an indication that these 3 proteins are TiO_2-NPS induced specifically.

In G5 (BPA treatment only), four proteins were found down-regulated in when compared to the Control (Fig. 4A). Protein actin-12 (ACT12) was considered as one of the reproductive actins and its expression in the root cap and pericycle tissues associated with root development (Cheng et al., 2017). The down-regulation of ACT12 was not consistent with our observation that root development was depressed in morphological analysis. This may be indicated that the impact of ACT12 down-regulation could be offset by other up-regulated proteins. The other 3 down-regulated proteins were 40 S ribosomal protein S17–3 (RS173, an mRNA binding protein), myrosinase 2 (BGL37, which may degrade glucosinolates to toxic degradation products (Islam et al., 2009)) and Beta-galactosidase 4 (BGAL4, which hydrolyzes para-nitrophenyl-beta-D-galactoside (Ahn et al., 2007)). Again, we noticed that RS173, BGL37, and BGAL4 were also found down-regulated in G2 vs. Control. As G2 has the same level of BPA as G5, it could be an indication that these 3 proteins are BPA induced specifically. Out of 12 SEDPs, seven up-regulated proteins were found G5 vs. Control, and 3 of them were plant growth-related proteins. They were cell division control protein 48 homolog E (CD48E, involved in cell division and growth process), chaperone protein dnaJ 2 (DNAJ2, played a continuous role in plant development), germin-like protein subfamily 2 member 4 (GL24, participated in the regulation of root development (Gaudet et al., 2011)). This indicated that in the response of BPA and TiO_2-NPS stress, plant primary root length would be shorter and more branched roots were observed in G1, G2, and G3 in comparison to the control (Fig. 1C). The other up-regulated proteins were ras-related protein RABA2c (RAA2C, intracellular vesicle trafficking and protein transport), chaperonin 60 subunit beta 2 (CPNB2, participates in protein refolding process), 60 S ribosomal protein L18a-3 (R18A3, an mRNA binding protein), and dehydrin Xero 2(XERO2, response to

water deprivation or abscisic acid). CD48E, DNAJ2, GL24, CPNB2, and XERO2 were also found up-regulated in G2 vs. Control (SI Table 4). Again, these 5 proteins could be induced by BPA specifically.

Besides the proteins that were aforementioned in G4 and G5, there were another 25 proteins, 13 up-regulated and 12 down-regulated, found significantly and differentially expressed in G2 as compared to the control (Fig. 4A). G2 contained the same BPA level as what was in G5 and the same TiO_2-NPS level as that in G4. Those 25 proteins could be resulting from the combining effects of BPA and TiO_2-NPS. Some proteins such as A0A384KEJ8 (a defense response protein (Zapata et al., 2016)), Myrosinase 4 (BGL34, for hydrolyzes sinigrin (Andersson et al., 2009)), protein sieve element occlusion B (SEOB, for phloem development (Anstead et al., 2012)), and probable plastid-lipid-associated protein 1 (PAP1, involved in light/cold stress (Youssef et al., 2010)) were found down-regulated, suggesting that the plant growth would have been negatively affected under the exposure of the contaminants at high concentrations and reflected in the plant heights and biomasses. However, the presence of these proteins did not result in significantly negative morphology outcomes (Fig. 1 E and F). Such observation suggested that the toxic effects of the co-existence of BPA and TiO_2-NPS at this concentration were not significant enough to cause the damage in growth or that the effects were offset by the growth enhanced effects by other up-regulated proteins. The up-regulated proteins found in G2 vs. control pertain to energy production and protein transportation. For example, Tubulin beta-6 chain (TBB6) is involved in microtubule cytoskeleton organization and microtubule-based process; Calmodulin-1 (CALM1) is involed in metal-binding (Gaudet et al., 2011); Ras-related protein RABA2a (RAA2A) is involed in intracellular vesicle trafficking and protein transport; Glyceraldehyde-3-phosphate dehydrogenase GAPCP2 (G3PP2) plays a specific role in glycolytic energy production (Muñoz-Bertomeu et al., 2010); 3-oxoacyl-[acyl-carrier-protein] synthase I (KASC1) catalyzes the condensation reaction of fatty acid synthesis (Gaudet et al., 2011). The G2 treatment stimulated the up-regulation of those protein suggesting that plant promote the ability of resource transportation and energy metabolism to overcome the stress and maintain or somehow enhance their growth.

3.3. KEGG pathways and interaction networks

To study SDEPs and their biological functions, KEGG pathways and interaction networks approaches were implemented by STRING analysis. In order to obtain an extended network, all proteins reported by Scaffold Q+ were taken into account (after the Benjamini-Hochberg procedure), including the less significant fold-changes, i.e. $\log_2$fold-change< 0.5. The STRING analysis of interaction networks are shown in Fig. 5. The roles of proteins in the core and the relationship between proteins were observed. With the higher concentration exposure of BPA and TiO_2-NPs, the interaction networks became more complex. Thirty three 33 clusters of interaction networks were identified in G1, 11 in G2, 2 in G3, 1 in G4, and 2 in G5 (details shown in Table S5).

The analysis illustrated that that *Arabidopsis* invoked more bioprocesses to deal with the stricter abiotic stresses compared to those groups with less BPA or TiO_2-NPs (G1 >G2 >G3 >G4/G5). As shown in Table 2, under the exposure of TiO_2-NPs alone (i.e. in G4), 2

affected KEGG pathways were glutathione metabolism, and starch and sucrose metabolism, which enhanced the plant growth at biomass and plant height, although the difference was not significant as shown in the previous morphology analysis. Meanwhile, under the circumstance of BPA exposure alone (i.e. in G5), 2 KEGG pathways were identified: ribosome and the metabolisms of protein processing in the endoplasmic reticulum. As the co-existence of BPA and TiO_2-NPs and the applied concentration got higher, the involved processes were various. 17 KEGG pathways were identified in G1, 5 pathways in G2, and 3 pathways in G3.

It should be noted that some individual proteins that affecting plant growth were not cited in the KEGG pathways and interaction networks. For instance, the up-regulated proteins may positively affect plant conditions such as GPLPC (egulation of protein phosphorylation), TTHL (regulation of cell growth by extracellular stimulus), RHM1 (regulation of cell proliferation), and HLB1 (root hair elongation) etc; and the down-regulated may negatively affect plant growth, such as DJ1A (regulation of cellular response to oxidative stress), UGE1 and EXPA4 (cell wall organization), and PATL1 (pollen tube growth). The finding suggests that the effects of BPA and TiO2-NPs on plant growth are complex and need more further studies (details shown in Table S6).

4. Conclusion

To understand the possible effects of biosolid application on agriculture, it is important to analyze the possible contaminants that coexist in biosolids. Using a model plant, *Arabidopsis thaliana*, and two commonly found contaminants, BPA and TiO_2-NPs, our finding showed that the plant germination and branch roots growth were enhanced under higher concentrations of BPA and TiO_2-NPs, while the primary root elongation was suppressed. There was no significant impacts on plant height and biomass once plants were mature under the levels of BPA and TiO_2-NPs tested in this research. In the comparative proteomics analysis, proteins of biological processes associated with root growth, plant development, and energy metabolism were found. Both positive and negative effects corresponding to the concentration of BPA and TiO_2-NPs were observed: such as regulation of cell proliferation (positive), root hair elongation (positive), cellular response to oxidative stress (negative), and cell wall organization (negative). Our comparative proteomics analysis also highlighted multiple biological processes, such as signaling, hormonal, and metabolic pathways which consequently lead to stability of plant growth and its stress adaptation. This indicates that when exposed to environmental stresses, plants will launch various biological processes to keep their normal growth. Plants seem to have a pearl of wisdom in their system to maintain a balance.

Overall, the evidence showed that under these environmentally relevant concentrations, the growth of *Arabidopsis thaliana* is not affected by the concurrent exposure to TiO_2 – NPs and BPA. Thus, in our study, the practice of applying biosolids in agriculture, especially contained BPA and TiO_2-NPS at the concentrations commonly found in the environment (i.e., less than 1000 μg/kg BPA and 100 mg/kg TiO_2-NPs) may not have significant impacts on plant growth and therefore might be an acceptable application for soil nutrient enhancement. Further examination is needed to have a comprehensive understanding of the

long-term impact (such as multigenerational study) of biosolids in agriculture application and across plant species.

Supplementary Material

Refer to Web version on PubMed Central for supplementary material.

Acknowledgments

The authors would like to thank the the UTEP Biomolecule Analysis and Omics Unit (BAOU) director, Dr. Igor C. Almeida, for services and facilities provided. The authors would like to acknowledge Dr. Jorge Gardea and Dr. Jose Hernandez at UTEP for their assistant in Greenhouse experiments. Special thanks to Frances Rangel, an undergraduate researcher supported by the UTEP BUILDing SCHOLARS Summer program supported by the National Institute of General Medical Sciences of the National Institutes of Health under linked Award Numbers RL5GM118969, TL4GM118971, and UL1GM118970. The content is solely the responsibility of the authors and does not necessarily represent the official views of the National Institutes of Health.

Funding Information

This project was supported by the Youth Talented Scientist Program for visiting scholars from the Fujian Academy of Agricultural Sciences, China. Grant supports included (1) Youth Talented Scientist Program (2018) of Fujian Academy of Agricultural Sciences (FAAS), (2) Special Project for Public Research Institutes of Fujian Province, 2020R1030005 and (3) Foreign Cooperation Projects of FAAS, DEC2020–01. Igor L. E. is supported by The University of Texas at El Paso Doctoral Excellence Fellowship. This work was also supported by Grant 5U54MD007592 from the National Institutes on Minority Health and Health Disparities (NIMHD), a component of the National Institutes of Health (NIH). W.-Y. Lee is partially supported by Grant 5SC1CA245675 from NIH.

References

Aguilera J, et al. , 2020. Nα-Acetylation of the virulence factor EsxA is required for mycobacterial cytosolic translocation and virulence: Nα-Acetylation of EsxA facilitates heterodimer separation. J. Biol. Chem 295, 5785–5794. [PubMed: 32169899]

Ahn YO, et al. , 2007. Functional genomic analysis of Arabidopsis thaliana glycoside hydrolase family 35. Phytochemistry 68, 1510–1520. [PubMed: 17466346]

Andersson D, et al. , 2009. Myrosinases from root and leaves of Arabidopsis thaliana have different catalytic properties. Phytochemistry 70, 1345–1354. [PubMed: 19703694]

Anstead JA, et al. , 2012. Arabidopsis P-protein filament formation requires both AtSEOR1 and AtSEOR2. Plant Cell Physiol. 53, 1033–1042. [PubMed: 22470058]

Bahmani R, et al. , 2020. The mechanism of root growth inhibition by the endocrine disruptor bisphenol A (BPA). Environ. Pollut 257, 113516. [PubMed: 31733969]

Bellani L, et al. , 2020. TiO2 nanoparticles in a biosolid-amended soil and their implication in soil nutrients, microorganisms and Pisum sativum nutrition. Ecotoxicol. Environ. Saf 190, 110095. [PubMed: 31869714]

Bonshtien AL, et al. , 2009. Differential effects of co-chaperonin homologs on cpn60 oligomers. Cell Stress Chaperon-.-. 14, 509–519.

Campos DA, et al. , 2020. Natural TiO2-Nanoparticles in Soils: A Review on Current and Potential Extraction Methods. Crit. Rev. Anal. Chem 1–21.

Chahardoli A, et al. , 2022. Uptake, translocation, phytotoxicity, and hormetic effects of titanium dioxide nanoparticles (TiO2NPs) in Nigella arvensis L. Sci. Total Environ 806, 151222. [PubMed: 34715233]

Chang AC, et al. , 2001. Developing human health-related chemical guidelines for reclaimed waster and sewage sludge applications in agriculture. World Health Organ. Eur. Environ. Bur 13.

Cheng CY, et al. , 2017. Araport11: a complete reannotation of the Arabidopsis thaliana reference genome. Plant J. 89, 789–804. [PubMed: 27862469]

Colón J, et al. , 2017. Producing sludge for agricultural applications. Innovative Wastewater Treatment Resource Recovery Technologies: Impacts on Energy. Econ. Environ

Corrales J, et al. , 2015. Global Assessment of Bisphenol A in the Environment: Review and Analysis of Its Occurrence and Bioaccumulation. Dose Response 13, 1559325815598308. [PubMed: 26674671]

Dixon DP, et al. , 2011. The Arabidopsis phi class glutathione transferase At GSTF2: binding and regulation by biologically active heterocyclic ligands. Biochem. J 438, 63–70. [PubMed: 21631432]

Fang Q, et al. , 2016. Enhanced bioconcentration of bisphenol A in the presence of nano-TiO2 can lead to adverse reproductive outcomes in zebrafish. Environ. Sci. Technol 50, 1005–1013. [PubMed: 26694738]

Feizi H, et al. , 2012. Impact of Bulk and Nanosized Titanium Dioxide (TiO2) on Wheat Seed Germination and Seedling Growth. Biol. Trace Elem. Res 146, 101–106. [PubMed: 21979242]

García-Santiago X, et al. , 2016. Risk assessment of persistent pharmaceuticals in biosolids: dealing with uncertainty. J. Hazard. Mater 302, 72–81. [PubMed: 26444489]

Gaudet P, et al. , 2011. Phylogenetic-based propagation of functional annotations within the Gene Ontology consortium. Brief. Bioinform 12, 449–462. [PubMed: 21873635]

Giudice BD, Young TM, 2011. Mobilization of endocrine-disrupting chemicals and estrogenic activity in simulated rainfall runoff from land-applied biosolids. Environ. Toxicol. Chem 30, 2220–2228. [PubMed: 21786314]

Gottschalk F, et al. , 2009a. Modeled environmental concentrations of engineered nanomaterials (TiO2, ZnO, Ag, CNT, fullerenes) for different regions. Environ. Sci. Technol 43, 9216–9222. [PubMed: 20000512]

Gottschalk F, et al. , 2009b. Modeled environmental concentrations of engineered nanomaterials (TiO2, ZnO, Ag, CNT, fullerenes) for different regions. Environ. Sci. Technol 43, 9216–9222. [PubMed: 20000512]

Guo J, Chen J-G, 2008. RACK1 genes regulate plant development with unequal genetic redundancy in Arabidopsis. BMC Plant Biol. 8, 108. [PubMed: 18947417]

Guo Y, et al. , 2019. Parental co-exposure to bisphenol A and nano-TiO2 causes thyroid endocrine disruption and developmental neurotoxicity in zebrafish offspring. Sci. Total Environ 650, 557–565. [PubMed: 30205345]

Hu X, Zhou QJC r, 2013. Health Ecosyst. Risks Graph. 113, 3815–3835.

Islam MM, et al. , 2009. Myrosinases, TGG1 and TGG2, Redundantly Function in ABA and MeJA Signaling in Arabidopsis Guard Cells. Plant Cell Physiol. 50, 1171–1175. [PubMed: 19433491]

Kim D, et al. , 2018. Effects of bisphenol A in soil on growth, photosynthesis activity, and genistein levels in crop plants (Vigna radiata). Chemosphere 209, 875–882. [PubMed: 30114736]

Laware S, Raskar S, 2014. Effect of titanium dioxide nanoparticles on hydrolytic and antioxidant enzymes during seed germination in onion. Int. J. Curr. Microbiol. Appl. Sci 3, 749–760.

Li X, et al. , 2018. A preliminary analysis of the effects of bisphenol A on the plant root growth via changes in endogenous plant hormones. Ecotoxicol. Environ. Saf 150, 152–158. [PubMed: 29274504]

Loeffler C, et al. , 2005. B1-phytoprostanes trigger plant defense and detoxification responses. Plant Physiol. 137, 328–340. [PubMed: 15618427]

Mahakham W, et al. , 2017. Nanopriming technology for enhancing germination and starch metabolism of aged rice seeds using phytosynthesized silver nanoparticles. Sci. Rep 7, 8263. [PubMed: 28811584]

Mahmoodzadeh H, et al., 2013. Effect of nanoscale titanium dioxide particles on the germination and growth of canola (Brassica napus).

Metsalu T, Vilo J, 2015. ClustVis: a web tool for visualizing clustering of multivariate data using Principal Component Analysis and heatmap. Nucleic Acids Res 43, W566–W570. [PubMed: 25969447]

Mohapatra DP, et al. , 2011. Occurrence of bisphenol A in wastewater and wastewater sludge of CUQ treatment plant. J. Xenobiotics 1.

Movafeghi A, et al. , 2018. Effects of TiO2 nanoparticles on the aquatic plant Spirodela polyrrhiza: Evaluation of growth parameters, pigment contents and antioxidant enzyme activities. J. Environ. Sci 64, 130–138.

Muñoz-Bertomeu J, et al. , 2010. The plastidial glyceraldehyde-3-phosphate dehydrogenase is critical for viable pollen development in Arabidopsis. Plant Physiol. 152, 1830–1841. [PubMed: 20107025]

Navarro E, et al. , 2008. Environmental behavior and ecotoxicity of engineered nanoparticles to algae, plants, and fungi. Ecotoxicology 17, 372–386. [PubMed: 18461442]

Petrie B, et al. , 2019. Assessment of bisphenol-A in the urban water cycle. Sci. Total Environ 650, 900–907. [PubMed: 30308864]

Philippe A, et al. , 2018. Characterization of the natural colloidal TiO2 background in soil. Separations 5, 50.

Shah T, et al. , 2021. Seed priming with titanium dioxide nanoparticles enhances seed vigor, leaf water status, and antioxidant enzyme activities in maize (Zea mays L.) under salinity stress. J. King Saud. Univ. -Sci 33, 101207.

Simonin M, et al. , 2021. Low mobility of CuO and TiO2 nanoparticles in agricultural soils of contrasting texture and organic matter content. Sci. Total Environ 783, 146952. [PubMed: 33866176]

Sun W, Zhou K, 2015. Adsorption of three selected endocrine disrupting chemicals by aquatic colloids and sediments in single and binary systems. J. Soils Sediment 15, 456–466.

Takeda M, et al. , 2008. Structure of the putative 32 kDa myrosinase-binding protein from Arabidopsis (At3g16450. 1) determined by SAIL-NMR. FEBS J. 275, 5873–5884. [PubMed: 19021763]

The Arabidopsis Genome, I., 2000. Analysis of the genome sequence of the flowering plant Arabidopsis thaliana. Nature 408, 796–815. [PubMed: 11130711]

Torri S, Alberti C, 2012. Characterization of organic compounds from biosolids of Buenos Aires city. J. Soil Sci. Plant Nutr 12, 143–152.

Verslycke T, et al. , 2016. Human health risk assessment of triclosan in land-applied biosolids. Environ. Toxicol. Chem 35, 2358–2367. [PubMed: 27552397]

Wang S, et al. , 2015a. Effects of bisphenol A, an environmental endocrine disruptor, on the endogenous hormones of plants. Environ. Sci. Pollut. Res Int 22, 17653–17662. [PubMed: 26150296]

Wang S, et al. , 2015b. Effects of bisphenol A, an environmental endocrine disruptor, on the endogenous hormones of plants. Environ. Sci. Pollut. Res 22, 17653–17662.

Wang Y, et al. , 2021. Soil-aged nano titanium dioxide effects on full-grown carrot: Dose and surface-coating dependent improvements on growth and nutrient quality. Sci. Total Environ 774, 145699. [PubMed: 33609834]

Weigel D, Glazebrook J, 2002. Arabidopsis: A Laboratory Manual. CSHL Press,.

Weir A, et al. , 2012. Titanium dioxide nanoparticles in food and personal care products. Environ. Sci. Technol 46, 2242–2250. [PubMed: 22260395]

Wu D, et al. , 2017. Influence of Bisphenol A on the transport and deposition behaviors of bacteria in quartz sand. Water Res. 121, 1–10. [PubMed: 28505529]

Yang Y, et al. , 2014. Metal and nanoparticle occurrence in biosolid-amended soils. Sci. Total Environ 485–486, 441–449.

Youssef A, et al. , 2010. Plant lipid-associated fibrillin proteins condition jasmonate production under photosynthetic stress. Plant J. 61, 436–445. [PubMed: 19906042]

Zapata L, et al. , 2016. Chromosome-level assembly of Arabidopsis thaliana Ler reveals the extent of translocation and inversion polymorphisms. Proc. Natl. Acad. Sci 113, E4052–E4060. [PubMed: 27354520]

Zheng L, et al. , 2005. Effect of nano-TiO 2 on strength of naturally aged seeds and growth of spinach. Biol. Trace Elem. Res 104, 83–91. [PubMed: 15851835]

Zhu F-D, et al. , 2012. Interaction of bisphenol A with dissolved organic matter in extractive and adsorptive removal processes. Chemosphere 87, 857–864. [PubMed: 22330311]

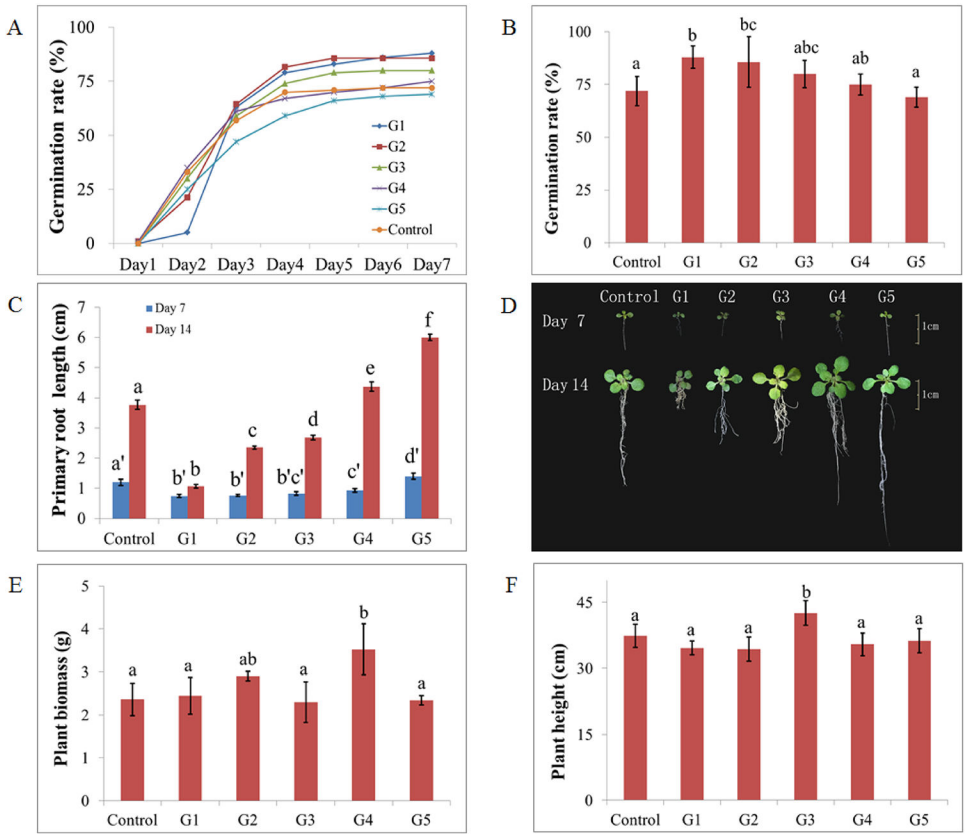

Fig. 1.

Plant response to different concentrations of BPA and TiO_2-NPs at germination (A and B), seedling (C and D), and mature stage (E and F). G1 to G5 represent 5 different treatments as indicated in Table 1. (A) Dynamic germination rate counted every day during the first 7 days (n = 100). (B) Seed's germination rate counted on 7th day after sown (n = 100). (C) Primary root length measured on day 7 and day 14 after seeds sown (n = 30). (D) Images of roots growth on day 7 and day 14. (E) Average plant height measured at the end of the 5th week (n = 30). (F) Total plant biomass (wet mass) determined upon harvest at the end of the 5th week. Values are average ± standard error. Same letters mean no statistical difference between treatments using one-way ANOVA ($p \leq 0.05$).

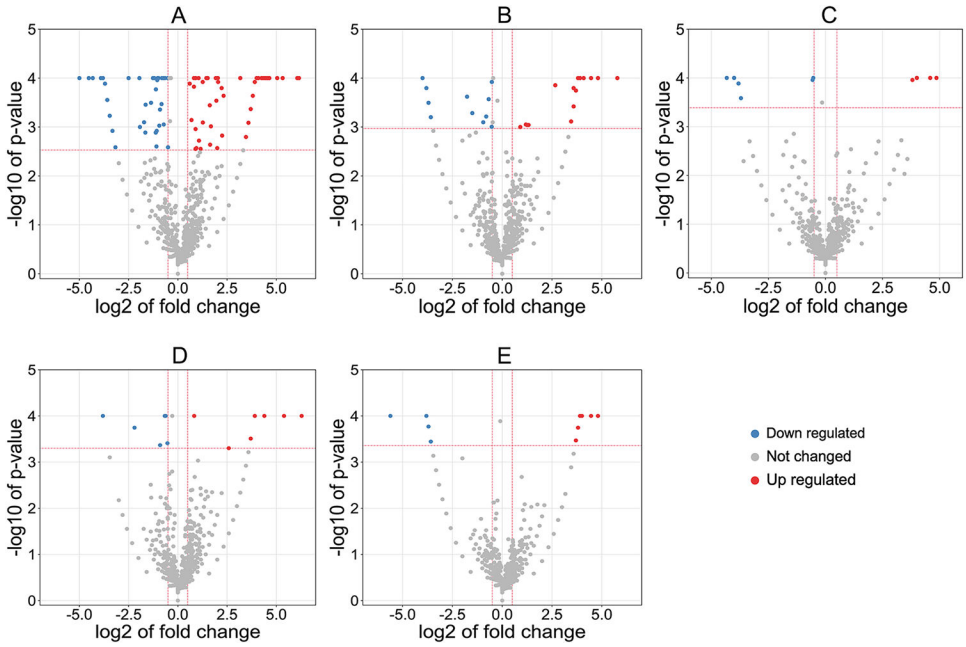

Fig. 2.

Volcano plots for the comparison between the treatment groups and control. A: G1 vs. Control, p-value < 0.00296, 64 up-regulated proteins and 52 down-regulated proteins, 116 SDEPs in total; B: G2 vs. Control, p-value < 0.00107, 19 up-regulated proteins and 19 down-regulated proteins, 38 SDEPs in total. C: G3 vs. Control, p-value < 0.00041, 5 up-regulated proteins and 7 down-regulated proteins, 12 SDEPs in total. D: G4 vs. Control, p-value < 0.00050, 7 up-regulated proteins and 7 down-regulated proteins, 14 SDEPs in total. E: G5 vs. Control, p-value < 0.00044, 7 up-regulated proteins and 5 down-regulated proteins, 12 SDEPs in total. Non-changed proteins were shown in gray color. The red color dots were indicative of up-regulated proteins and the blue color dots were down-regulated proteins. The cutoff values of Log2 of fold change were set at ± 0.5.

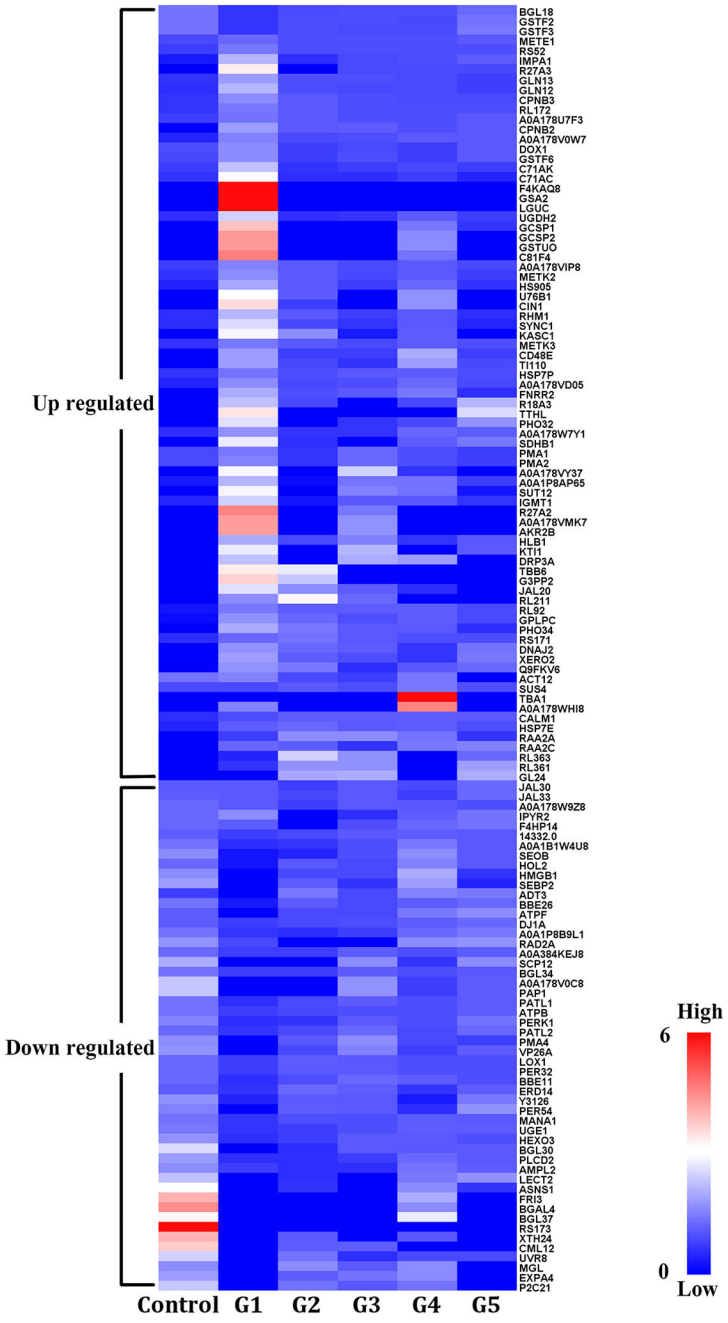

Fig. 3.

Heat map of significant differentially expressed proteins. The colors in the heat map indicate the relative abundance of proteins (fold changes compared to the average spectrum counts of each protein expressed in all groups). The color gradient from blue to red indicates the degree of expression from no expression to the high expressions. Specific proteins in the heatmap are listed in Table S2.

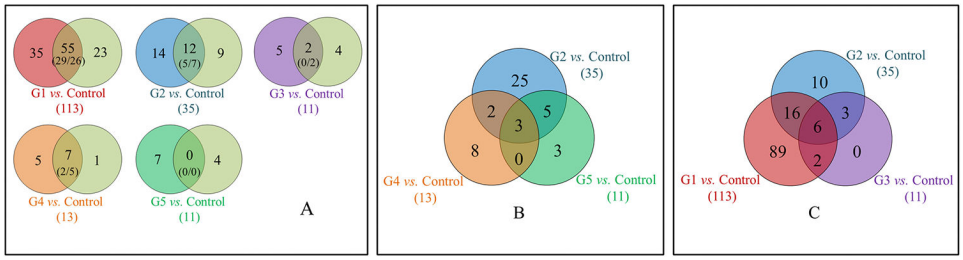

Fig. 4.

Venn diagram of significant differentially expressed proteins (SDEPs) identified. (A) All treatment groups compared to control. Numbers in the overlap areas represented the SDEPs being up-regulate (the left number) and down-regulate proteins (the right number). (B) Comparison among 3 treatments that contained both BPA and TiO_2-NPs or only BPA or TiO_2-NPs at the same corresponding concentrations: G2 vs. Control, G4 vs. Control and G5 vs. Control. (C) Comparison among three treatments that contained both BPA and TiO_2-NPs at different concentrations. G1 vs. Control, G2 vs. Control and G3 vs. Control.

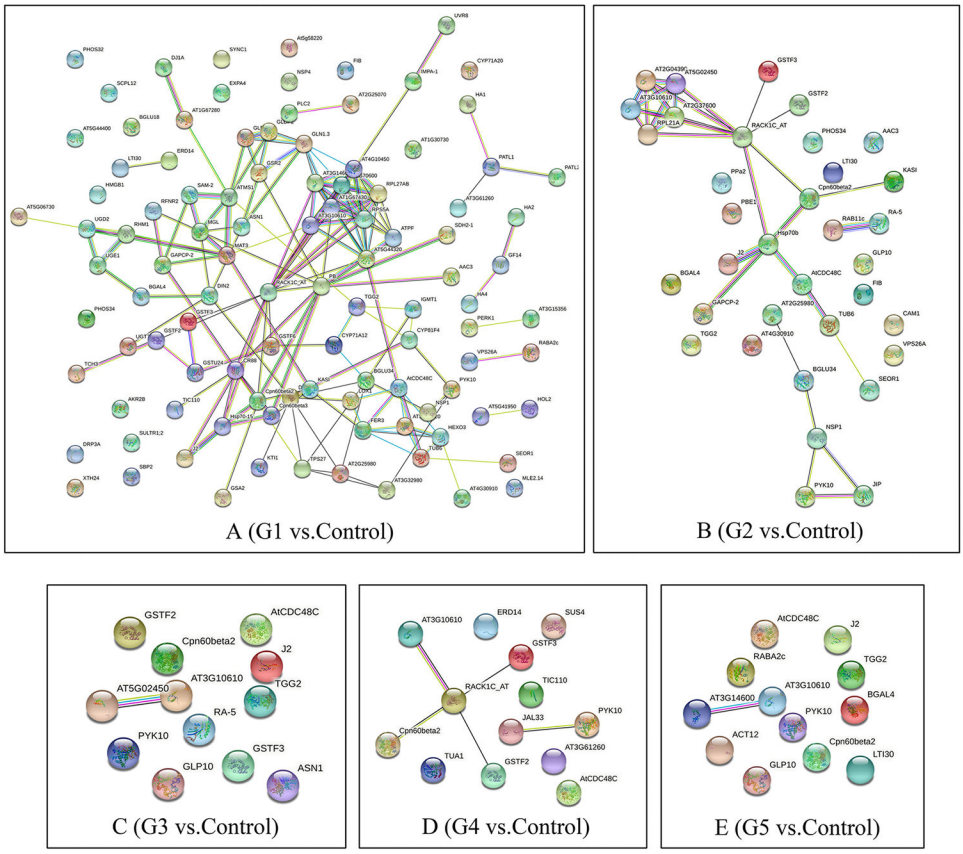

Fig. 5.

Interaction networks of significant proteins. The higher concentrations of BPA and TiO_2-NPs, the more complexed the interaction networks (G1 > G2 > G3 > G4 > G5). 33clusters of interaction networks were identified in G1, 11 in G2, 2 in G3, 1 in G4, and 2 in G5 (Table S5).

Table 1

BPA and TiO_2-NPs concentrations in experimental treatments and control.

Groups	Concentration of contaminants	
	BPA	**TiO_2-NPs**
G1	1000 μg·kg^{-1}	100 mg·kg^{-1}
G2	100 μg·kg^{-1}	10 mg·kg^{-1}
G3	10 μg·kg^{-1}	1 mg·kg^{-1}
G4	0	10 mg·kg^{-1}
G5	100 μg·kg^{-1}	0
Control	0	0

Table 2

KEGG Pathways of the significant differentially expressed proteins.

Group of Significant Proteins	KEGG Pathway	Description	Proteins Involved	Count in Network[a]	Strength[b]	False Discovery Rate[c]
G1 v.s. Control (116 proteins)	ath00190	Oxidative phosphorylation	PMA1; SDHB1; PMA4; PMA2; ATPF; ATPB	6 of 149	1.03	0.0007
	ath00195	Photosynthesis	FNRR2; ATPF; ATPB	3 of 76	1.02	0.012
	ath00220	Arginine biosynthesis	GLN12; GLN13	2 of 36	1.17	0.0284
	ath00250	Alanine, aspartate and glutamate metabolism	GLN12; GLN13; ASNS1	3 of 49	1.21	0.0063
	ath00270	Cysteine and methionine metabolism	MGL; METK3; METK2; METE1	4 of 114	0.97	0.0063
	ath00380	Tryptophan metabolism	BGL34; C71AC; BGL37	3 of 53	1.17	0.0063
	ath00450	Selenocompound metabolism	MGL; METE1	2 of 18	1.47	0.0107
	ath00480	Glutathione metabolism	GSTF6; GSTUO; GSTF3; GSTF2; AMPL2	5 of 98	1.13	0.00076
	ath00511	Other glycan degradation	HEXO3; MANA1	2 of 19	1.44	0.0109
	ath00520	Amino sugar and nucleotide sugar metabolism	UGE1; HEXO3; RHM1; UGDH2	4 of 131	0.91	0.0079
	ath00630	Glyoxylate and dicarboxylate metabolism	GLN12; GCSP2; GLN13; GCSP1	4 of 75	1.15	0.0026
	ath00910	Nitrogen metabolism	GLN12; GLN13	2 of 43	1.09	0.0371
	ath00940	Phenylpropanoid biosynthesis	BGL23; PER32; BGL30; PER54	4 of 167	0.8	0.0136
	ath01100	Metabolic pathways	UGE1; G3PP2; FNRR2; HEXO3; GLN12; GCSP2; METK3; PLCD2; BGL23; GLN13; SDHB1; UGDH2; PER32; ASNS1; GSA2; BGL30; METK2; AMPL2; GCSP1; PER54; METE1; KASC1; TTHL	25 of 1899	0.54	1.87E-06
	ath01110	Biosynthesis of secondary metabolites	G3PP2; GCSP2; METK3; BGL23; SDHB1; PER32; ASNS1; GSA2; BGL30; METK2; GCSP1; PER54; METE1	13 of 1063	0.51	0.0026
	ath01230	Biosynthesis of amino acids	G3PP2; GLN12; METK3; GLN13; METK2; METE1	6 of 244	0.81	0.0027
	ath03010	Ribosome	R27A2; RL172; R27A3; RS173; RS52; R18A3; RL92	7 of 318	0.76	0.0026
G2 v.s. Control (38 proteins)	ath00380	Tryptophan metabolism	BGL34; BGL37	2 of 53	1.47	0.0124
	ath00480	Glutathione metabolism	GSTF3; GSTF2; AMPL2	3 of 98	1.38	0.0064
	ath03010	Ribosome	RS171; RL361; RS173; RL363	4 of 318	0.99	0.008
	ath04141	Protein processing in endoplasmic reticulum	HSP7E; CD48E; DNAJ2	3 of 205	1.06	0.0124
	ath04144	Endocytosis	RAA2A; HSP7E; VP26A	3 of 142	1.22	0.008
G3 v.s. Control (11proteins)	ath00480	Glutathione metabolism	GSTF3; GSTF2	2 of 98	1.67	0.0093
	ath03010	Ribosome	RS173; RL363	2 of 318	1.16	0.0304

Group of Significant Proteins	KEGG Pathway	Description	Proteins Involved	Count in Network[a]	Strength[b]	False Discovery Rate[c]
	ath04141	Protein processing in endoplasmic reticulum	CD48E; DNAJ2	2 of 205	1.35	0.0196
G4 v.s. Control (14 proteins)	ath00480	Glutathione metabolism	GSTF3; GSTF2	2 of 98	1.63	0.0100
	ath00500	Starch and sucrose metabolism	BGL23; SUS4	2 of 147	1.46	0.0110
G5 v.s. Control (12 proteins)	ath03010	Ribosome	RS173; R18A3	2 of 318	1.16	0.0373
	ath04141	Protein processing in endoplasmic reticulum	CD48E; DNAJ2	2 of 205	1.35	0.0320

[a]Count in Network:The first number indicates how many proteins in the network are annotated with a particular term. The second number indicates how many proteins in total (in the network and in the background) have this term assigned.

[b]Strength: Log10(observed/expected). This measure describes how large the enrichment effect is. It's the ratio between i) the number of proteins in the network that are annotated with a term and ii) the number of proteins that we expect to be annotated with this term in a random network of the same size.

[c]False Discovery Rate: This measure describes how significant the enrichment is. The numbers shown are p-values corrected for multiple testing within each category using the Benjamini–Hochberg procedure.